IMPROVING REACTIVITY AGAINST TARGET ORGANOTHIOPHOSPHATES VIA ACTIVE-SITE DIRECTED MUTAGENESIS OF A BACTERIAL PHOSPHOTRIESTERASE

A Thesis

by

TYLER EDWARD GITHENS

Submitted to the Office of Graduate Studies of
Texas A&M University
in partial fulfillment of the requirements for the degree of

MASTER OF SCIENCE

Approved by:

Chair of Committee,	Frank M. Raushel
Committee Members,	Hays Rye
	Tadhg Begley
Head of Department,	Gregory D. Reinhart

December 2012

Major Subject: Biochemistry

ABSTRACT

Phosphotriesters, also known as organophosphates (OP), represent a class of toxic compounds first synthesized in Germany. Enzymatic removal of harmful insecticides and breakdown products is a promising alternative to skimming or dredging. Wild type bacterial phosphotriesterase (PTE) was screened against 7 agricultural organophosphates: coumaphos, chlorpyrifos, fenitrothion, temephos, profenofos, pirimiphosmethyl and diazinon. The initial results laid the groundwork for a mutagenesis study to investigate the determining factors in enzyme reactivity. Coumaphos is hydrolyzed more efficiently than any other target by the wild type cobalt enzyme ($k_{cat}/K_m = 2 \times 10^7\ M^{-1}s^{-1}$). Coumaphos, fenitrothion and chlorpyrifos had the lowest K_m values from the initial screen and were targets for steady state kinetic characterization of active site mutants. Site directed mutagenesis of binding sites was conducted and the most reactive point mutants, F132G, F132V and S308G, were used as backgrounds for subsequent mutation. Seven active site double mutants: F132G/S308G, F132G/S308T, F132V/S308G, F132V/S308T, F132G/I106T, F132V/I106T and G308/W309 were purified to homogeneity for kinetic characterization. The double mutant G308/F132V enhanced chlorpyrifos reactivity relative to the wild type enzyme. This enhancement of reactivity is proposed to result from conformational rearrangement following substrate bond hydrolysis.

ACKNOWLEDGEMENTS

My education and training was the result of invaluable assistance from departmental professors and colleagues and most importantly my research advisor, Dr. Frank Raushel. His patience and attention to detail are remarkable and I am indebted to him for his support in completing my thesis project. This work was made possible by the training and advice provided by my lab mates and particularly Dr. Andrew Bigley. Support from loved ones despite understanding little of my work has lifted me during periods of frustration. I want to acknowledge the collegiality of the graduate student population. Conversations outside of classrooms, break rooms and libraries have helped to solve problems and provide perspective during stressful times.

Dissertations by Dr. Dumas and Dr. Chen-Goodspeed were invaluable sources of information for PTE physical and kinetic properties. Mutant proteins (F132G, I106G, S308G) prepared by Dr. Chen-Goodspeed and pet20 constructs prepared by Dr. Eman Ghanem (M317K, F132V, I106T) were used for preparation and kinetic characterization of mutant enzymes with target substrates and paraoxon.

NOMENCLATURE

PTE	Phosphotriesterase from *Pseudomonas diminuta*
OP	Organophosphates
FNT	Fenitrothion
CPF	Chlorpyrifos
COU	Coumaphos

TABLE OF CONTENTS

Page

LIST OF FIGURES

Page

LIST OF TABLES

Page

CHAPTER I

INTRODUCTION TO THE BACTERIAL PHOSPHOTRIESTERASE

A research group working in an I.G. Farben laboratory run by Dr. Gerhard Schrader began synthesizing a new class of organophosphorus and fluorophosphate insecticides in 1936 as a replacement for nicotine [1]. Several of these compounds were discovered to exhibit strong toxicity against humans. Large chemical munitions plants were erected during World War II to produce organophosphates for military use. The discovery of organophosphate (OP) production by the allies after WWII ushered in a new era of military science in the United States. US production and storage of sarin continued from the 1950s until a 1969 moratorium, with resumption of production in 1986 [2]. US chemical weapon production was halted in 1993 and 90% of remaining stockpiles destroyed since the UN Chemical Weapons convention came into effect in 1997 [3] .

Organophosphates became popular as insecticides in an era when DDT use was still common. More persistent organochlorine and organofluorine insecticides were replaced with organophosphorus insecticides; many of the most popular OP insecticides are still produced in excess of 10^7 tons/year (EPA factsheet, 2008). Environmental effects from residual contamination become a grave concern once phosphotriesters were discovered to function as potent acetylcholinesterase inhibitors. Acetylcholine typically binds an active site serine with release of acetate and choline following hydrolysis. OP binding at the serine residue generates a tetrahedral intermediate which collapses to

displace the OP leaving group. The bound phosphate prevents regeneration of the catalytic hydroxyl group. Several of the original organophosphates (parathion, paraoxon, tabun, sarin) are good substrates for the wild type phosphotriesterase (PTE) from *Pseudomonas diminuta*. Reactivity (k_{cat}/K_m) is orders of magnitude higher with paraoxon and parathion than with the more toxic nerve agents tabun and sarin [4, 5].

Despite such a short history of organophosphate chemical synthesis, enzyme-mediated hydrolysis of paraoxon approaches diffusion-limited rates (k_{cat}/K_m (paraoxon) $\sim 10^8$ M^{-1} s^{-1}). Contamination from banned insecticides is an environmental concern and enzymatic degradation represents a viable means of detoxification [6]. Runoff from organophosphate-treated soil is toxic to marine life and birds as well as insects [7]. Agricultural production has been dramatically enhanced by removal of crop-damaging pests, but the environmental cost of insecticide use has not yet been fully realized. Organophosphate insecticides increase hemocyte count and inhibit lytic enzyme function in target organisms [8]. The selected compounds for this study are all acetylcholinesterase inhibitors that likely form covalent adducts with an active site serine [9]. Unmitigated acetylcholine buildup impairs nervous system function in a lethal fashion. Resistance to OP can occur via modulation of acetylcholinesterase at the genetic and functional levels. Elevated transcription levels, increased protein production, enhanced selectivity towards the native substrate, and improved overall enzymatic reactivity have all been characterized in OP-resistant insects [10].

PTE is a member of the amidohydrolase superfamily and contains a characteristic $(\alpha/\beta)_8$ barrel structural fold. The enzyme exhibits broad substrate specificity with a large

group of toxic phosphotriesters. The preferred substrate, paraoxon, contains a p-nitrophenol leaving group. Many organothiophosphate compounds with aromatic leaving groups have been characterized as substrates for PTE. The enzyme binding sites tolerate phenyl rings with a wide range of substitutions [11]. Several nerve agents with alkyl (VX, tabun) and fluoride (sarin, soman) leaving groups are also substrates [12]. PTE facilitates hydrolysis of P-O, P-F, P-S, and P-CN bonds but hydrolyzes P-O bonds most rapidly [13]. Three insecticides, chlorpyrifos, coumaphos and fenitrothion, were chosen as targets for active site mutagenesis.

Coumaphos is the largest of the target insecticides and contains a 6-chloro, 7-methyl coumarin ring with a diethoxy thiophosphate group. Coumaphos was first registered for use in 1958 as a commercial insecticide/acaricide and is most commonly used to control anthropod pests which thrive near farm-raised cattle, swine, sheep, horse and goat populations. Coumaphos is a cholinesterase inhibitor and is registered only for direct animal treatment. The United States Department of Agriculture (USDA) requires inborne livestock from Mexico to swim through vats filled with coumaphos solution to control ticks carrying bovine piroplasmosis (Texas Cattle Fever) [14]. Coumaphos is highly toxic by oral (TC I) and inhalation (TC II) exposure and moderately toxic via dermal exposure (TC III). Residual dietary exposure in 1996 was expected to be 39% of the Reference Dose (RfD) for the US population and 73% of the RfD for non-nursing babies, a concentration deemed benign over a 70-year lifetime. Coumaphos can be metabolized and excreted within a week of exposure and is a class E carcinogen (non-carcinogenic to humans) [14].

Chlorpyrifos is the second largest of the target compounds and has a 3,4,6-chloro pyridine leaving group attached to a dimethoxy thiophosphate head group. Chlorpyrifos was first registered for use in 1965 by Dow Chemical Company and is one of the most frequently used insecticides in the world [15]. It is registered for use as an insecticide, miticide, and acaricide and is used to control soil-borne pests. An estimated 10 million pounds of chlorpyrifos are applied for agricultural purposes in the US annually [16]. Chlorpyrifos has been banned for residential use but is approved for use in the agricultural sector, most commonly for corn, alfafa, and cotton. Widespread application is permitted due to the relatively benign effects on humans. However, persistent toxicity is observed in representative species of crustacean and avian wildlife [17]. Chlorpyrifos is the least water-soluble compound selected for catalytic enhancement.

Fenitrothion is a broad-spectrum insecticide first introduced for commercial use in 1959 [18]. Although treated wheat is imported into the United States, fenitrothion's only registered use in the US is for child resistant, containerized ant and roach baits [19]. Exposure to fenitrothion via food or drinking water is not considered a major health risk. Fenitrothion exhibits low toxicity against mammals and is excreted rapidly with no signs of bioaccumulation. Buildup of reactive oxygen species (ROS) is a potentially dangerous side effect of organophosphate insecticide use [20]. Fenitrothion has the highest solubility in water of any of the target compounds. Coupled with the increased danger of ROS products, fenitrothion persistence in the environment is particularly troubling. Biomolecules which bind the parent compound may not recognize breakdown products, necessitating a multi-pronged approach for removal.

The substrates tested in the initial screen (Figure 1) all contain methoxy or ethoxy phosphoryl side groups and an aromatic alcohol leaving group. The leaving groups of the target organothiophosphates are: 6-chloro, 7-methyl coumarin ring from coumaphos, m-methyl p-nitrophenol of fenitrothion, and 3,4,6-chloro pyridine ring of chlorpyrifos. Fenitrothion contains methoxy phosphoryl groups; the other two targets contain ethoxy groups. The preferred substrate contains a diethoxy phosphate head group and a singly conjugated phenolic leaving group. Although the preferred moiety has been elucidated, the relative importance of leaving group size and polarity for catalysis is not completely understood. Perhaps the smaller leaving groups of chlorpyrifos and fenitrothion permit unproductive binding, while the coumarin ring of coumaphos must be aligned for hydrolysis in order to effectively bind PTE.

PTE is a metal-dependent hydrolase with broad substrate specificity. Enzymatic P-O bond cleavage proceeds in an associative fashion with inversion of stereochemistry at the phosphorus center [21]. An activated hydroxide molecule is positioned for attack of the bound substrate, typically a phosphotriester, thiophosphate or phosphorothiolate [22]. PTE contains a binuclear metal center with a bridging water or hydroxide molecule. Metal-substrate coordination displaces the bridging water or hydroxide molecule and polarizes the phosphoryl bond for hydroxide attack [23] (Figure 2). Water then displaces the phosphate product and regenerates the catalytic hydroxide [23, 24].

Organophosphate structures

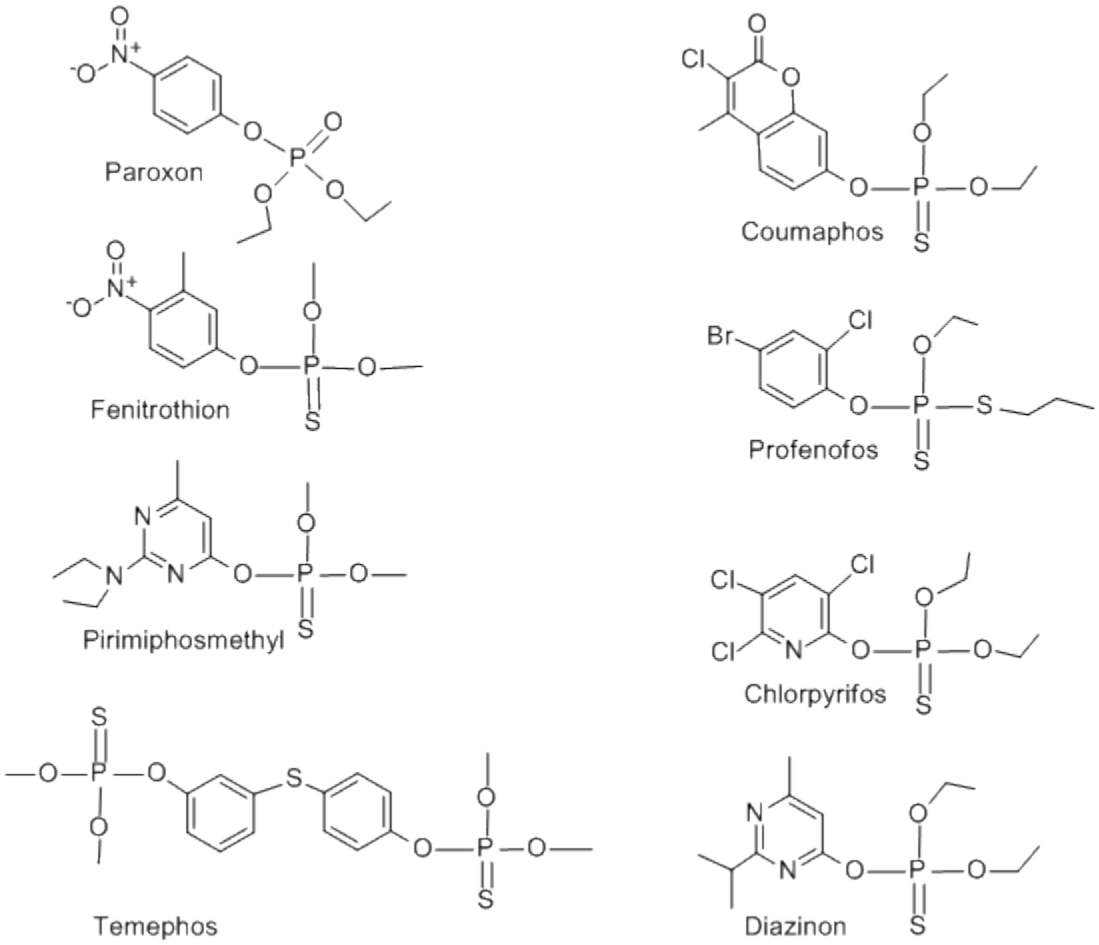

Figure 1: *Organophosphate structures*. Chemical structures of the organophosphates tested in this study. The four diethyl thiophosphates are shown on the right while the three methyl thiophosphate compounds are shown on the left with paraoxon, the preferred substrate.

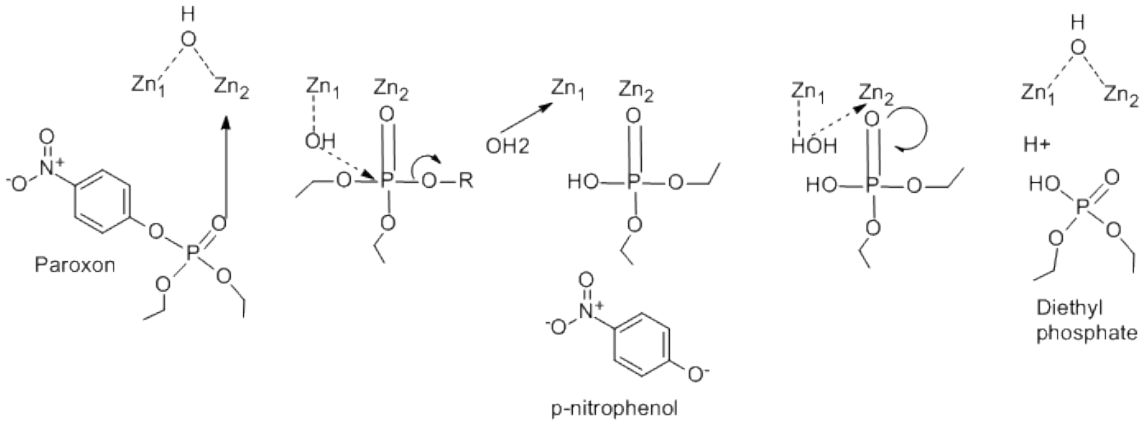

Figure 2: *Schematic for paraoxon hydrolysis*. Schematic for paraoxon hydrolysis by the wild type Zn/Zn phosphotriesterase.

The active site architecture seen in PTE is found in other enzymes in the amidohydrolase superfamily. The pentavalent α-zinc ion is coordinated to two histidines, one aspartate, and one carboxylated lysine residue, while the tetravalent β-zinc atom is coordinated to two histidines and the bridging carboxylated lysine residue [25] (Figure 3). An X-ray structure of PTE bound to a prochiral substrate analog revealed the presence of three distinct subsites for substrate binding: the leaving group pocket, the large group pocket and the small group pocket [25].

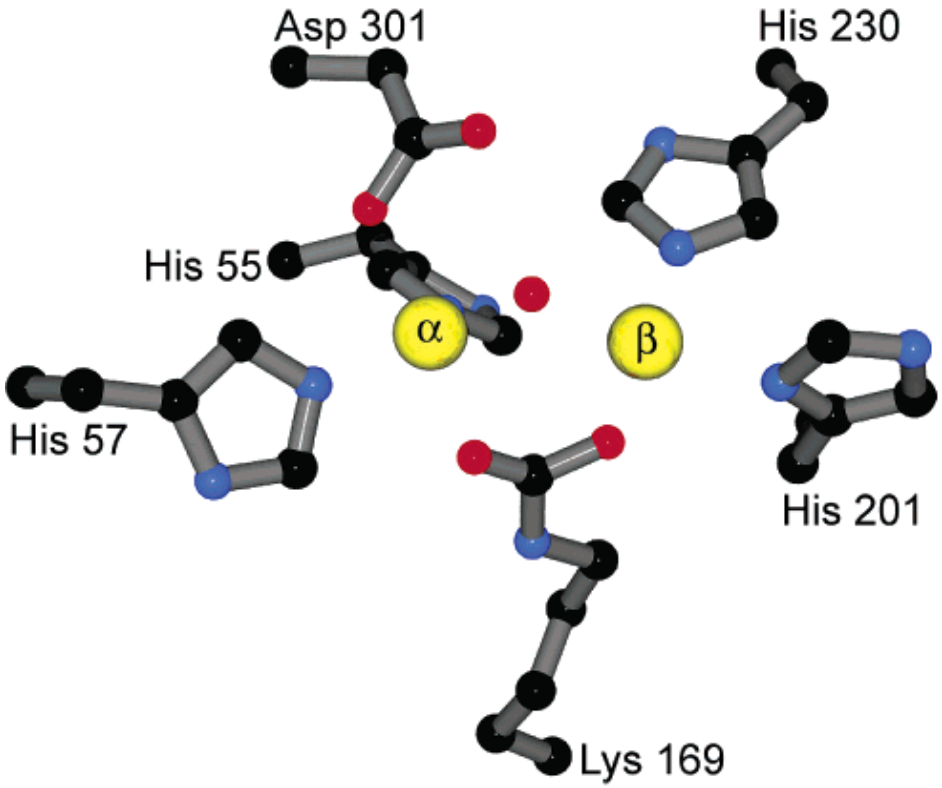

Figure 3: *Active site metal coordination*. Metal coordination within the active site of phosphotriesterase involves five direct amino acid contacts (Figure from [23]). The active site histidine cluster is typical for the amidohydrolase superfamily. Lys 169 bridges both active site metals while Asp301 is involved in proton transfer.

Protonation of the leaving group is unnecessary; protons can be shuttled from the active site towards the surface of the protein by an aspartate-histidine-aspartate triad (Figure 4) [23]. Although produced natively by several soil bacteria, PTE's best substrates are synthetic chemicals. This rapid adaptation could be explained by enzyme promiscuity, but the absence of selective pressure against OP contact as well as a lack of known native substrates for PTE complicates any explanation for retention of the

plasmid-borne gene. Rapid depletion of free phosphate molecules may have necessitated phosphate scavenging as a means for survival.

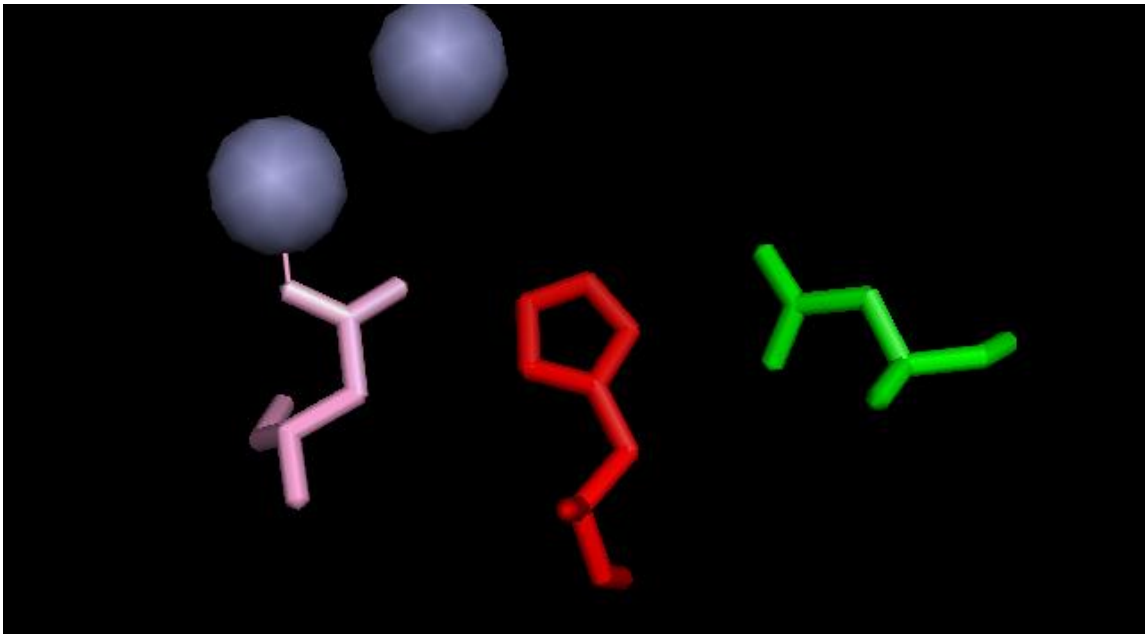

Figure 4: *Proton shuttling in the active site*. An amino acid triad shuttles protons away from the binuclear metal center (Zn^{++} ions shown in gray) to the metal-coordinated Asp301 (pink), then His254 (red) and finally Asp233 (green).

Previous work has shown that the rate-limiting step in hydrolysis of thiophosphate substrates with aromatic leaving groups can be predicted based on the pKa of the leaving group. For thiophosphates with leaving group pKa values below ~8.5, the rate limiting step is due to a conformational change or binding event as determined from a Brønsted analysis [11]. The replacement of the hard oxygen atom with a soft sulfur atom likely affects the metal-ion interaction, the polarity of the thiophosphate bond, and potentially affects formation of transition state structures [26].

Mutagenesis studies have demonstrated PTE's pliability for enzyme redesign [27-29]. Mutation of F132 to alanine, for instance, abolishes stereoselectivity between chiral substrates, presumably by facilitating the removal of large aromatic leaving groups from the enzyme active site [30]. This finding highlights how drastically reactivity can vary between point mutants. Point substitutions at many positions within the active site permit efficient turnover of paraoxon ($k_{cat}/K_m \geq 10^6$ M^{-1} s^{-1}). However, technical considerations preclude kinetic characterization of mutants which greatly increase K_m with the target compounds. While paraoxon's water solubility is in the millimolar range, the target compounds are nearly insoluble in water. Reactions for which the K_m value greatly exceeded the solubility limit of the target compound were not kinetically characterized.

CHAPTER II

MATERIALS AND METHODS

Cell culture growth

1 liter cultures of Terrific Broth containing 12 g tryptone, 24 g yeast extract, 4 g glycerol, 2.3 g KH_2PO_4 and 12.5 g K_2HPO_4 were prepared for bacterial cell growth. The PTE gene from *Pseudomonas diminuta* was cloned into a BL21 (DE3α) E. coli expression vector under the control of a T7 promoter for protein expression. 50 uL of competent cells were electroporated with $\simeq$ 25 ng of plasmid prior to overnight growth on LB-ampicillin plates. A 5 mL LB culture with antibiotic was grown for 12 hours after picking one of the resulting colonies. Culture flasks were subsequently inoculated from the 5 mL cultures and grown an additional 12 hours prior to addition of IPTG. Cultures were grown at a final IPTG concentration of 1 mM for 24 hours prior to cell harvesting. Cell pellets which were not immediately prepared for purification were stored in 50 mL falcon tubes at -80 ^{o}C.

Protein preparation

Five four-minute rounds of sonication were performed on ice with intermittent 10 minute breaks (Branson Sonifier 450, 50% duty cycle, 6.5-7 output control). Following sonication, cells were spun at 13,000*g* for 10 minutes and the supernatant saved for protamine sulfate precipitation. 0.45 g of protamine sulfate were dissolved in 20 mL of purification buffer and added dropwise via a separatory funnel to the supernatant over a period of 30 minutes at 4^{o}C. After protamine sulfate precipitation, the solution was spun

at 13,000*g* for 10 minutes. The resulting supernatant was subjected to ammonium sulfate precipitation (36.1 g/100 mL) with stirring over the course of 30 minutes at 4°C. Following ammonium sulfate precipitation the sample was spun at 13,000*g* for 20 minutes. The resulting pellet (< 1 g) was suspended in 5 mL of purification buffer before filtration through a 0.45 μm Millipore filter. The filtered sample was then injected onto a 120 mL HiLoad 16/60 Superdex 200 FPLC column and eluted in 50 mm HEPES, 100 μM $CoCl_2$, pH. 8.5 aqueous buffer at 1.5 mL/min. The resulting gel filtration fractions are tested for activity against paraoxon, and a 3-4 fraction peak of activity was further purified using a DEAE-Sephadex column washed with elution buffer prior to packing. The enzyme elutes quickly at pH 8.5 due to its high pI and separates from the remaining *E. coli* proteins. Fifteen fractions were collected from the DEAE column for analysis via SDS-PAGE. The chosen fractions were pooled and flash frozen in liquid nitrogen prior to storage at -80° C.

Kinetic analysis

All steady-state kinetic reactions were conducted in 50 mM CHES, pH 9.0 with no more than 20% organic solvent in aqueous solution. Enzyme is diluted into elution buffer prior to reaction and added last to initiate all reactions unless otherwise indicated. The substrates, however, were not diluted directly from organic solvent into the reaction mixture. In order to reduce turbidity the organophosphate substrates were added from a stock concentration of 40-50% methanol to the reaction mixture. Solubility limits in organic solvent/water mixtures were determined visually by cloudiness or precipitation after pipette mixing or vortexing. Difference absorbance spectra comparing the

product(s) of enzymatic hydrolysis and substrate were generated in order to select a wavelength for observation of product formation. A second wavelength at which neither substrate nor product absorbs was monitored during kinetic assays to detect nonspecific changes in absorbance. Quantitative analysis of solvent effects on enzyme function using paraoxon as a substrate were performed to determine the potential effect of different organic solvents on k_{cat} and K_m (Figure 5).

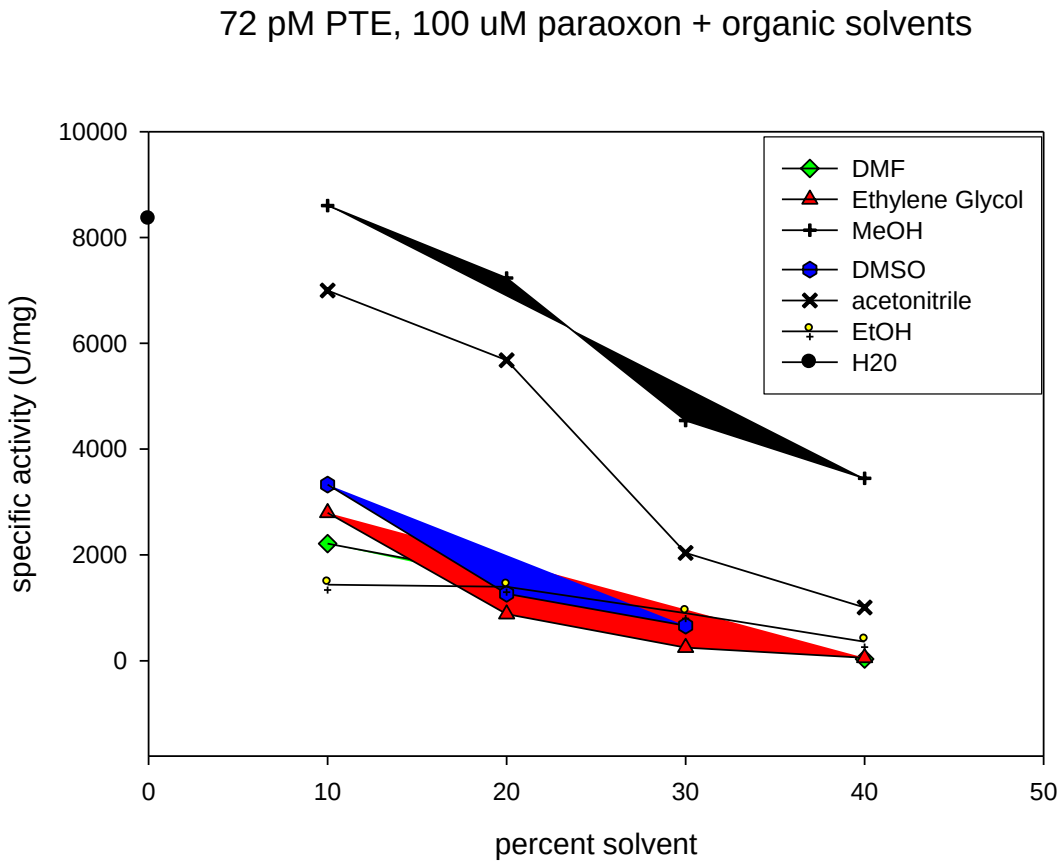

Figure 5: *PTE activity in various organic solvents*. Specific activity range against paraoxon in a variety of selected organic solvents. Acetonitrile and methanol have a relatively minor effect at concentrations $\leq$ 20%. Ethanol diminishes specific activity even at low concentrations, while methanol has a minimal effect up to 20%.

Site directed mutagenesis

DNA constructs were prepared via Stratagene's Quikchange Site-Directed Mutagenesis kit. Mutagenic primers were ordered through the Gene Technology Laboratory at Texas A&M University (GTL). Conditions used for gene amplification were as follows:

1:	95.0°C for 4:00
2:	95.0°C for 0:45
3:	55 °C - 65 °C for 0:30
4:	68.0°C for 6:00
5:	Go to 2, 18 times
6.	68.0°C for 12:00
7.	4.0°C for ever

Annealing temperatures between 5-12 °C below T_m were used depending on T_{extend}-T_m. Instances where this value was negative resulted in more truncated transcripts, necessitating a lower annealing temperature. 50 µL reactions were prepared in autoclaved water with 20-25 ng of template DNA, 125-200 ng of sense primer, 125-200 ng of antisense primer, 1 µL of dNTP mix (10 mM each), and 1 µL of Agilent *PfuTurbo* DNA polymerase (2.5 U/ µL). The elongation time of six minutes was chosen due to the size of the pet20 construct (1024 bp insert + ~ 2.5 kBp plasmid). PCR products were cooled to 37°C before adding 1 µL of DpnI and pipette mixing. Following a 1 min spin at 11,000*g* the PCR reactions are incubated overnight at 37°C. PCR cleanup was performed prior to transformation into XL-1 Blue competent cells. Resulting colonies from overnight growth on LB-amp plates were picked for 14-18 hours of growth and DNA was prepared for sequencing PCR with a Qiagen Spin miniprep kit. The 6 µL PCR sequencing reactions contained 2 µL of Big Dye (purchased from GTL), 2 µL of

plasmid, and 2 μL of T7 primer (terminator or promoter). Both forward and reverse sequencing reactions were performed for each plasmid. Completed sequencing PCR reactions were diluted to 20 μL with autoclaved water, loaded onto GTL supplied PCR cleanup columns and spun at 1,300*g* for 3 minutes. The flow-through was dried over vacuum for 1 hour and sent for sequencing at the GTL. Six of the seven double mutants prepared and described herein were prepared by introducing single mutations into one of three point mutant constructs generated by Dr. Eman Ghanem (I106T, S308G, S308T). The seventh double mutant was prepared from WT PTE plasmid. Conditions for cell growth, protein expression and protein purification were identical for mutant and wild type protein.

CHAPTER III

RESULTS

WT characterization

Wild type enzyme with cobalt was prepared as described previously and purified to $\geq$ 90% homogeneity [12]. Experimentally determined k_{cat} and K_m values for hydrolysis of paraoxon were 10,900 s^{-1} and 0.11 mM respectively, with a k_{cat}/K_m value of 9.6 x 10^7 $M^{-1}s^{-1}$ (Table 1). Kinetic characterization of the seven organophosphate compounds yielded a wide array of k_{cat} (7.5 ~ 1,200 s^{-1}) and K_m (20 ~ 2,000 μM) values (Table 1). The initial kinetic screen was carried out in 10-20% methanol depending on solubility limits for each compound. Many of the substrates had K_m values in excess of their solubility limit in 20% MeOH. However, increasing the concentration of organic solvent negatively affects enzyme function (Figure 5).

Coumaphos and chlorpyrifos both had lower K_m values than paraoxon. While chlorpyrifos hydrolysis was comparatively slow, coumaphos was hydrolyzed more rapidly than any other target (Table 1). Chlorpyrifos and coumaphos are the two least soluble compounds from the initial screen; the Michaelis constant for the wild type enzyme is roughly equivalent to the solubility limit in 20% methanol for both. Diazinon and pirimiphosmethyl both have calculated K_m values above the tested substrate range. While diazinon has a k_{cat}/K_m value comparable to fenitrothion and the second highest k_{cat} value of the targets, it was not chosen as a target for enhanced catalysis. The large Michaelis constant is likely indicative of weak binding and solubility limitations make

fenitrothion a more attractive target. Profenofos contains two scissile bonds: a phosphoester linkage and a butyl thioester bond (Figure 2). All other targets contain thiophosphate head groups, but profenofos is an oxon. The comparatively high k_{cat} value is due to increased reactivity of the phosphate head group compared to the thiophosphate head groups of the other compounds.

The catalytic rate constant for the wild type PTE with coumaphos is 1,200 $\pm$ 150 s^{-1}. All other OP substrates tested in this study were hydrolyzed at rates between 10~350 s^{-1}. WT PTE (Co^{2+}/ Co^{2+}) hydrolyzed five compounds rapidly ($k_{cat}/K_m > 10^5$ M^{-1} s^{-1}) and coumaphos most efficiently ($k_{cat}/K_m > 10^7$ M^{-1} s^{-1}). The three compounds with the lowest K_m values (fenitrothion, coumaphos and chlorpyrifos) were selected as targets for enhanced catalysis via site-directed mutagenesis. A recent directed evolution study using selection against a methylcoumarinyl substrate analogue generated a mutant enzyme with a k_{cat}/K_m value nearly an order of magnitude higher than the wild type enzyme [31]. Coumaphos and chlorpyrifos vary only in leaving group, but fenitrothion has two O-methyl phosphoryl side groups (Figure 2).

Compound Name	MeOH (%)	[S] range (μM)	K_m (μM)	k_{cat} (s^{-1})	k_{cat}/K_m (s^{-1} M^{-1})
Paraoxon	0	8.35 - 622	110 ± 6	10,900 ± 200	9.6×10^7
Coumaphos	15	2.0 - 50	57 ± 10	1200 ± 140	2.1×10^7
Profenofos	15	5 - 200	200 ± 60	160 ± 30	8.0×10^5
Chlorpyrifos	20	1.0 - 25	18 ± 5	11 ± 1.7	6.1×10^5
Diazinon	18	100 - 700	1,900 ± 600	360 ± 100	1.9×10^5
Fenitrothion	15	15 - 375	150 ± 40	26 ± 3.0	1.7×10^5
Pirimiphosmethyl	15	4.0 - 94	210 ± 90	7.6 ± 2.4	3.6×10^4
Temephos	20	-	-	-	-

Table 1: *WT PTE kinetic profile with target organophosphates*. All reactions were run in 50 mM CHES, pH 9.0 and initiated by addition of enzyme. Purified enzyme (WT, Co/Co) was stored and diluted in 50 mM HEPES, pH 8.5 prior to addition. Molar extinction coefficients were calculated from absorbance difference spectra for substrate and hydrolysis product(s).

Characterization of the active site mutants

Proteins with one asterisk (*) in front of their name were expressed and purified from DNA constructs made by Dr. Eman Ghanem. Proteins with two asterisks (**) were purified previously by Dr. Chen-Goodspeed and stored at -80 ^oC for at least 10 years. All kinetic reactions for mutant enzymes were performed in 20% methanol. k_{cat}/K_m values without individual values for k_{cat} and K_m were calculated via linear fitting or Eadie-Hofstee analysis (Tables 2-5). All other values were determined by fitting to a single rectangular hyperbola fit in Sigma Plot.

Paraoxon hydrolysis

F132G, S308G, and F132V/I106T all hydrolyze paraoxon at least as efficiently as the wild type enzyme as determined by k_{cat}/K_m (Table 2). S308G/Y309W reduced k_{cat} 5-fold and had a k_{cat}/K_m value more than 30-fold lower than wild type. Most of the

characterized mutants had significantly higher K_m values, but F132G, F132V, and S308G all had K_m values less than 3-fold higher than the wild type enzyme. All other mutants had K_m values at least 5-fold higher. A resulting variant from a directed evolution study with paraoxon selection (F132L/I106T) hydrolyzed paraoxon 4 fold faster (k_{cat}) than the starting wild type enzyme but had a K_m value roughly 19-fold higher [31]. F132V/I106T has a k_{cat} value more than 9-fold greater than wild type and a K_m value just less than 9-fold higher. F132V/I106T has a k_{cat} 3-fold higher than F132G/I106T and half as large a Michaelis constant. The difference in hydrophobicity between these glycine and valine double mutants may account for the 5-fold difference in k_{cat}/K_m for paraoxon hydrolysis.

PTE variant	k_{cat} (s^{-1})	K_m (μM)	k_{cat}/K_m ($M^{-1} s^{-1}$)
WT	10,870 ± 188	113 ± 6	9.6×10^7
**F132G	21,600 ± 660	216 ± 22	1.5×10^8
**S308G	40,600 ± 2180	261 ± 45	1.5×10^8
F132V/I106T	103,000 ± 5,600	880 ± 190	1.2×10^8
**I106G	27000 ± 1700	535 ± 87	5.0×10^7
*F132V	14,560 ± 850	320 ± 38	4.5×10^7
**I106G/F132G/H257Y	22,200 ± 1770	863 ± 102	2.6×10^7
F132G/I106T	34,800 ± 4900	1700 ± 560	2.0×10^7
S308G/Y309W	2240 ± 100	740 ± 90	3.0×10^6

Table 2: *Paraoxon hydrolysis by PTE mutants*. Glycine substitution at positions 132 and 308 improved k_{cat}/K_m roughly 50% compared to wild type.

Coumaphos hydrolysis

Two point mutants and one double mutant (S308G, F132G, S308G/Y309W) had lower Michaelis constants than the wild type enzyme, but all three mutants drastically

reduced turnover (Table 3). F132V, which had the same K_m value as the wild type enzyme, had a k_{cat} value roughly 3-fold lower than wild type. F132V had by far the highest k_{cat} value and hydrolyzed coumaphos 22-fold faster than F132G. Pairing this mutation with S308G or S308T reduced k_{cat} and dramatically increased K_m compared to the F132V point mutant. S308G had the second highest k_{cat} of the point mutants, and the same k_{cat} as the double mutant F132V/S308G. This double mutant, however, had a K_m value more than 5-fold higher than either constituent point mutation. S308T substitution in the double mutants reduced reactivity relative to the point mutants.

PTE variant	k_{cat} (s^{-1})	K_m (μM)	k_{cat}/K_m ($M^{-1} s^{-1}$)
WT	1190 ± 140	57 ± 11	2.1×10^7
*F132V	380 ± 40	53 ± 10	7.2×10^6
**F132G	17 ± 6.0	8.0 ± 9.0	2.0×10^6
**S308G	80 ± 10	40 ± 11	2.0×10^6
S308G/F132V	-	-	3.0×10^5
S308T/F132V	-	-	1.3×10^5
S308G/Y309W	3.4 ± 0.4	40 ± 8.0	8.6×10^4
S308T/F132G	-	-	6.6×10^3

Table 3: *Coumaphos hydrolysis by PTE mutants*. The wild type enzyme hydrolyzes the coumarinyl thiophosphate analogues more efficiently than all of the active site mutants.

Chlorpyrifos hydrolysis

F132V/S308G had the highest k_{cat}/K_m value of any mutant enzyme characterized for CPF hydrolysis, roughly four times higher than the wild type enzyme (Table 4). F132G, F132V, and S308G all had similar k_{cat}/K_m values for chlorpyrifos hydrolysis, roughly 3-fold lower than the wild type enzyme. Low solubility and comparatively slow

turnover necessitated linear fitting or Eadie-Hofstee plots to estimate k_{cat}/K_m for CPF hydrolysis with most active site mutants. F132V/S308G hydrolyzes CPF at least as efficiently as the wild type enzyme, but with no detectable rate below 15 μM. The S308G point mutant improved k_{cat} as compared to the wild type enzyme, but dramatically increased the Michaelis constant. Y309 and F306 interact directly with the chloro-conjugated pyridine leaving group following hydrolysis. The hydroxyl group at position 308 may delocalize the resulting oxyanion and/or hydrogen bond the pyridine ring nitrogen. F132V and S308G are equally reactive, but appear to affect catalysis in an unrelated manner. Replacement of the phenyl ring with the isopropyl side group of valine removes bulk from the leaving group site, while S308G mutation permits productive orientation of the leaving group, Y309 and F306.

PTE variant	k_{cat} (s^{-1})	K_m (μM)	k_{cat}/K_m ($M^{-1} s^{-1}$)
S308G/F132V	-	-	2.6×10^6
WT	11.2 ± 1.7	18.3 ± 5.1	6.1×10^5
**F132G	-	-	2.3×10^5
**S308G	50 ± 39	270 ± 220	1.9×10^5
*F132V	-	-	1.9×10^5
**I106G	-	-	1.5×10^5
F132V/I106T	-	-	1.0×10^5
F132G/I106T	-	-	6.0×10^4
S308G/Y309W	-	-	6.9×10^4

Table 4: *Chlorpyrifos hydrolysis by PTE mutants*. F132V/S308G hydrolyzes the pyridine substrate more efficiently than the wild type protein.

Fenitrothion hydrolysis

Fenitrothion was hydrolyzed significantly more efficiently by the wild type enzyme than any of the tested mutants (Table 5). The two best variants (I106G/F132G/H257Y I106G) both contained I106G mutations and possessed nearly identical kinetic parameters. However, I106T substitution abolished activity in two double mutants. F132V had the second highest k_{cat}/K_m of the tested point mutants and S308G the third. Pairing these mutations reduced reactivity when compared with either point mutant. Interestingly, S308T/F132V undergoes substrate inhibition and has no detectable rate of hydrolysis at substrate concentrations above 100 μM. A closed conformation for PTE has been observed both in substrate free and Michaelis-complex crystal structures, which indicates that substrate binding does not induce this closed conformation (21). After substrate binding, a conformational change to accommodate transition state structures is necessary for efficient catalysis. Threonine mutation at position 308 could make the initial conformational change following hydrolysis rate limiting due to its proximity to Y309, which is in position to directly interact with the nascent leaving group.

PTE variant	k_{cat} (s^{-1})	K_m (μM)	k_{cat}/K_m (M^{-1} s^{-1})
WT	41 ± 7	110 ± 30	3.8×10^5
**I106G/F132G/H257Y	31 ± 10	559 ± 220	5.5×10^4
**I106G	31 ± 9	577 ± 204	5.4×10^4
*F132V	-	-	1.6×10^4
**S308G	4.6 ± 1.4	618 ± 239	7.4×10^3
**F132G	5.3 ± 2.1	1000 ± 672	5.3×10^3
S308G/F132V	1.74 ± 0.8	400 ± 280	4.4×10^3
S308G/Y309W	-	-	2.8×10^3
F132V/I106T	0.11 ± .02	78 ± 42	1.4×10^3
F132G/I106T	0.04 ± .01	50.9 ± 31.5	786
S308T/F132G	< 0.02	-	-
S308T/F132V	[S] inhibition (100 μM)	[S] inhibition (100 μM)	[S] inhibition (100 μM)

Table 5: *Fenitrothion hydrolysis by PTE mutants*. The wild type enzyme hydrolyzes the m-methyl, p-nitrophenol thiophosphate substrate much more efficiently than the active site mutants.

CHAPTER IV

DISCUSSION

The discovery of enzymes with OP activity shortly after initiation of chemical synthesis is intriguing. Could the answer to bioremediation of environmentally toxic chemicals already exist in the fields of treated soil? Is PTE unique in its ability to degrade insecticides or rather made unique by its discovery? The finding that enzymes with parathionase and paraoxonase activity exist in both mammalian and bacterial organisms would seem to favor the latter. The $(\alpha/\beta)_8$ protein fold is found throughout biology; the fold is almost exclusively for enzymes [32]. Active sites are found at the C-terminal end of the barrel and typically include a phosphate-binding motif. Such a diverse set of reactions are catalyzed by this structural class of enzymes that it typifies the "one fold-many functions" paradigm [32].

PTE's ability to degrade OP would appear to favor divergent evolution from an ancestral protein as explanation for its function. However, PTE was never incorporated into the genome of the soil bacteria from which it was isolated [33]. Identical genes were discovered on dissimilar plasmids originating from separate organisms. If divergent evolution is the mechanism by which phosphotriesterase activity originated, one would not expect what appears to be a conserved horizontal gene transfer event without selective pressure such as acquired antibiotic resistance [34]. OP exposure is toxic towards insects, birds, fish and mammalian species, but bacteria do not produce acetylcholinesterase, an essential protein for nervous system function and OP target.

PTE degrades paraoxon and several other organophosphates more rapidly than any known wild type enzyme. Even the worst substrate from the initial screen has a catalytic efficiency (k_{cat}/K_m) > 10^4 M^{-1} s^{-1}. Binding of the phosphate moiety likely occurs in very similar fashions between the thiophosphate substrates. A Brønsted analysis for the dependence of log Vmax on leaving group pKa indicates that bond cleavage for thiophosphate substrates with a leaving group pKa $\leq$ 8.5 is not rate limiting (Figure 6) [11]. Product removal is the predicted rate limiting step for the selected targets (COU, CPF, FNT). Mutation of leaving group residues is intended to weaken the interaction between product-like transition state structures of the aromatic leaving group product and the active site.

The three selected targets vary in their phosphoryl group identity (fenitrothion contains methoxy R groups; coumaphos and chlorpyrifos have ethoxy R groups) as well as their leaving groups. Since there was no enzymatic bias towards substrates with ethoxy R groups in the initial screen, the leaving group is predicted to determine reactivity. Differentiating between the reasons for tight binding of the targets could be explained by the size, hydrophobicity and pKa of the aromatic leaving groups. The m-methyl, p-nitrophenol leaving group for FNT is suspected to adopt similar conformations to p-nitrophenol during its passage through the active site. Methylation could have a chemical effect on the adjacent nitro group, alter substrate orientation, or possibly introduce a steric clash for one of the transition states. The other two targets have leaving groups dissimilar to the preferred p-nitrophenol, but pKa values such that bond cleavage is not rate limiting.

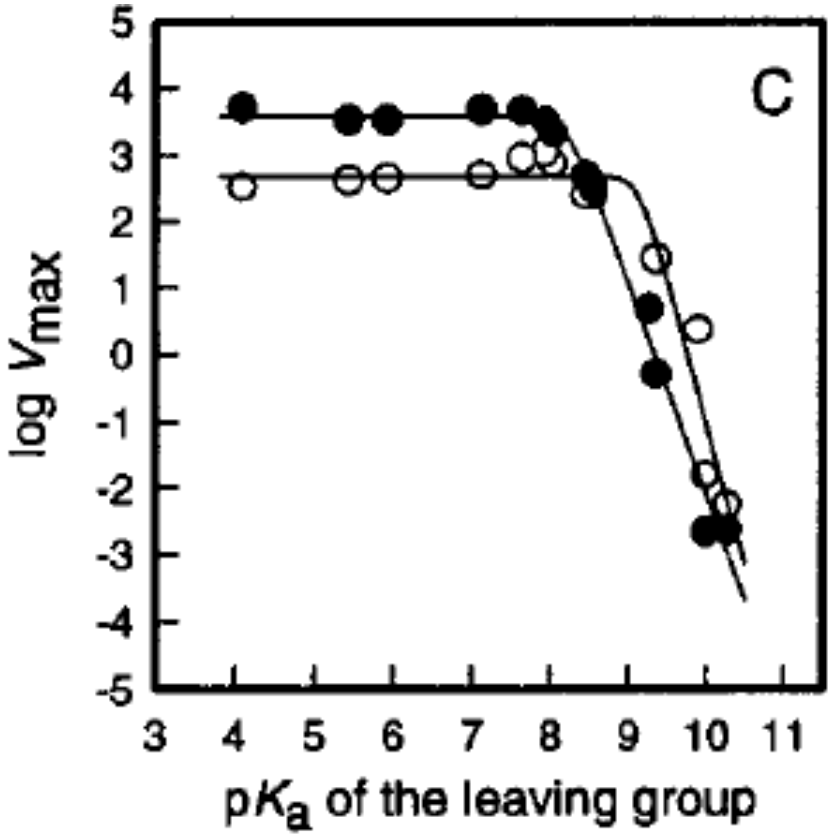

Figure 6: *Brønsted analysis of phosphate and thiophosphate substrates*. A Brønsted plot for PTE-mediated hydrolysis of a series of phosphate (black circles) and thiophosphate substrates (white circles) supports binding or conformational change as the rate limiting step for substrates with a leaving group pKa below 8.5 (Figure from [11]).

Recent studies utilizing DNA shuffling and directed evolution have identified residues in or near the active site amenable to substitution [27, 31, 35] (Figure 7). This approach is especially appropriate given the rapid natural evolution of the enzyme. A PTE variant with a 725-fold improvement in k_{cat}/K_m for chlorpyrifos, as determined by a

Lineweaver-Burk plot, was generated via DNA shuffling and plate screening with chlorpyrifos [36]. Three point mutants, F132G, F132V, and S308G, exhibited broad substrate specificity. Positions 132 and 308 were chosen as the first two sites for a series of active site double mutants. F132A has previously been shown to increase the k_{cat} for Rp enantiomers while having little to no effect on k_{cat} for the Sp enantiomers of chiral substrates [30]. It is expected that such a mutation will not impair hydrolysis of achiral substrates. For substrates whose catalysis is limited by product removal, reducing steric constraints within the leaving group subsite should aid hydrolysis. Residues in close proximity to the binuclear metal center were not considered for mutagenesis so as not to perturb the chemical environment for phosphoester bond cleavage.

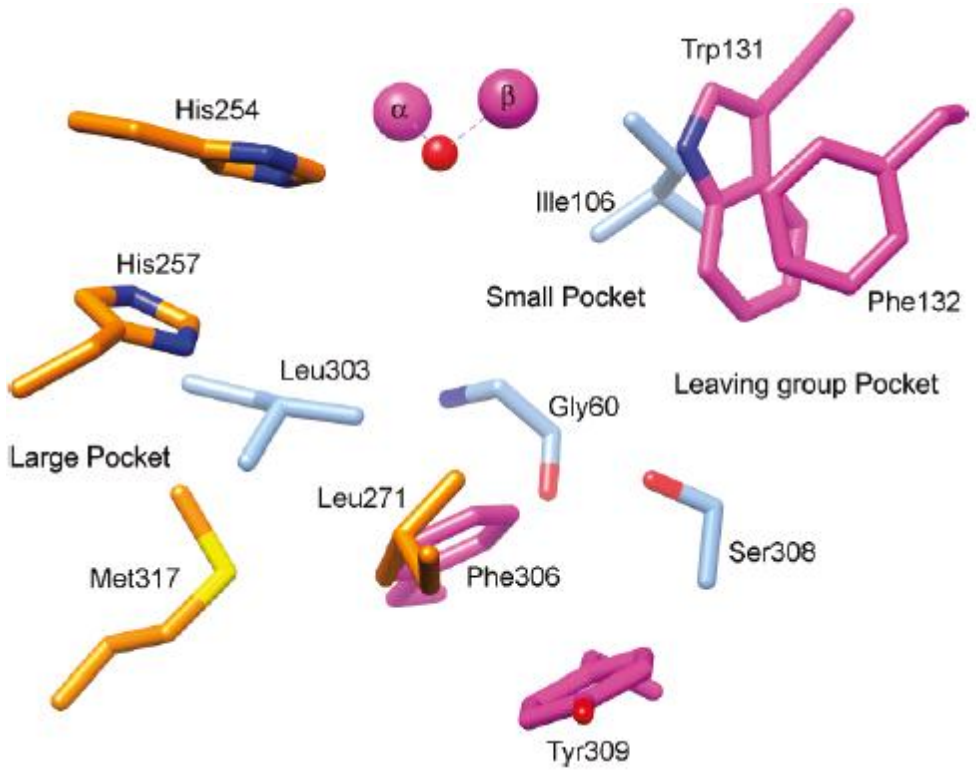

Figure 7: *The 12 active site residues of PTE* [12]. Purple residues (F306 & Y309, W131 & F132) comprise the leaving group pocket, blue residues (G60, I106, L303, S308) comprise the small group pocket, and orange residues (H254, H257, L271, M317) comprise the large group pocket. After the phosphate group binds at the large group pocket, the scissile P-O bond is lengthened and oriented for SN_2-type attack by an activated hydroxide molecule.

The point mutant I106T is known to reduce PTE's affinity for paraoxon, but an isolated mutant variant with a k_{cat} five-fold higher than WT against paraoxon contained I106T in addition to other mutations (F132V, S308A, and Y309W) [31]. What aspect of these mutations enhances catalysis? There seem to be two functional pairs of mutations acting in concert to improve reactivity. S308 and Y309 are positioned at the interface between the large subsite and the leaving group subsite [37]. Proton substitution for the serine hydroxyl and indole substitution for the tyrosine phenol group increases

hydrophobicity at this junction. Y309 and F306 appear to form a swinging door from the leaving group site (Figure 8). The G308 and W309 mutations may enhance catalysis by guiding the aromatic substituent of the substrate to the leaving group subsite after bond cleavage (Figure 9). The second pair of functional mutations, I106T and F132V, could widen the leaving group channel by introducing a hydrogen bonding partner for W131 and eliminating the bulk of the benzene R group. I106 is hydrogen bonding distance from both His57 and Trp131 in the metal-containing enzyme (Figure 10) [37]. Taken together, these four mutations enlarge the leaving group subsite channel while increasing hydrophobicity at the junction between the large subsite and the entrance to the leaving group site.

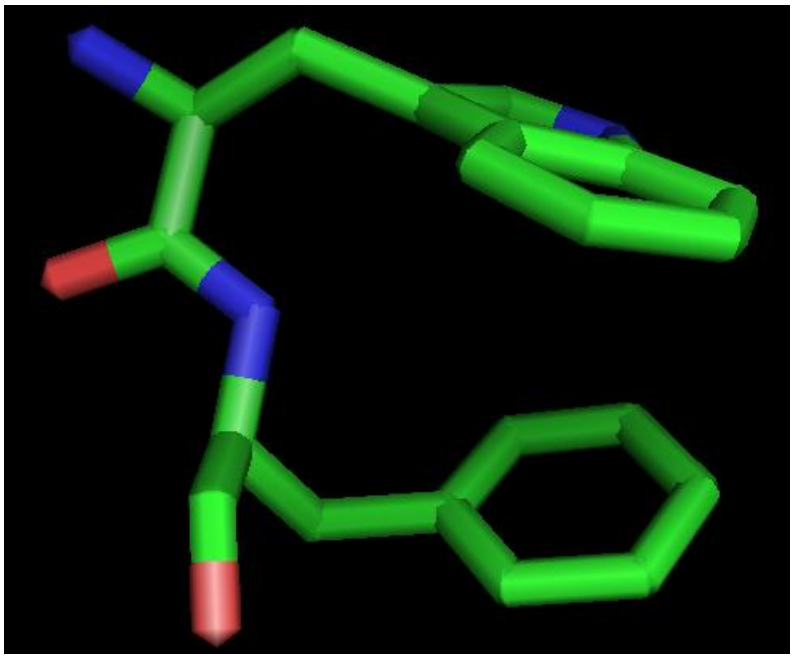

Figure 8: *The exit from the leaving group site*. F132 (bottom) and W131 (top) sit near the exit from the leaving group site. Alanine substitution for phenylalanine abolishes PTE stereoselectivity [30]. The importance of hydrophobic contribution to substrate binding at position 131 (top) was deduced from a previous mutagenesis study [38].

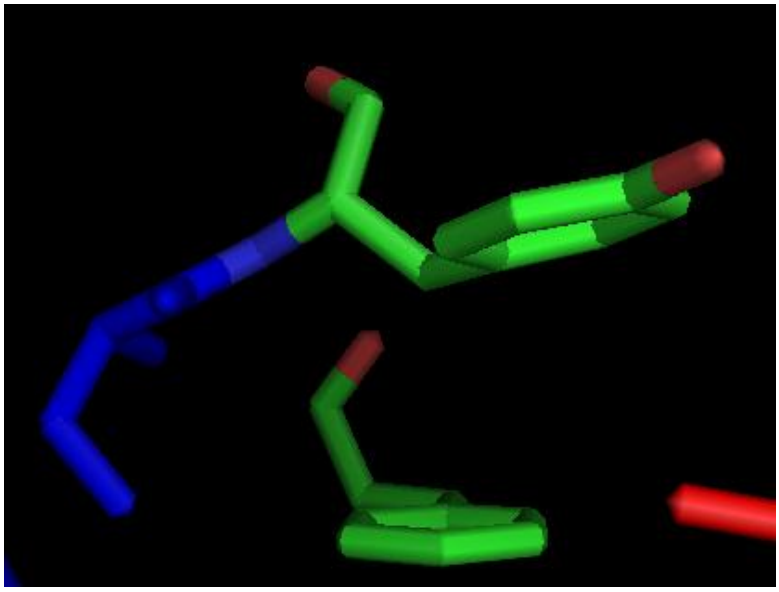

Figure 9. *S308 and Y309 form the small group/leaving group junction*. The interface between the small group pocket and the leaving group pocket is shown here. The blue residue S308 is attached to Y309.

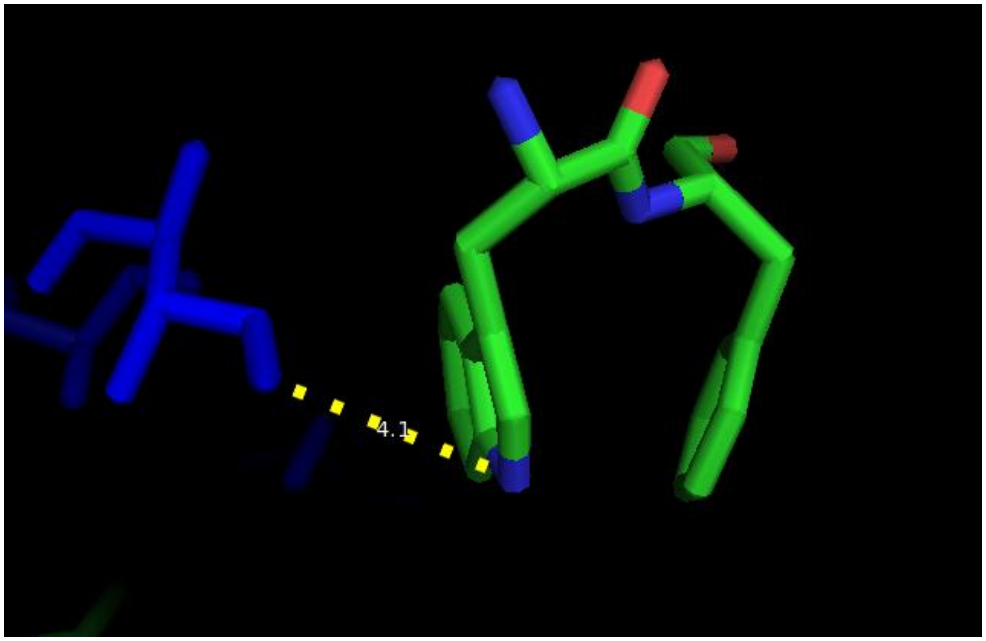

Figure 10. *I106, W131, and F132 sit near the active site exit*. The blue residue in the foreground is I106, while the two aromatic compounds (shown in green) are W131 and F132. I106T mutants were prepared to test whether a potential H-bond interaction with W131 could improve catalysis.

S308G/Y309W dramatically reduced activity against all targets (k_{cat}/K_m roughly 32 fold lower with paraoxon, 244 fold lower with COU, 9 fold lower with CPF, and 136 fold lower with FNT) compared to the wild type enzyme. Y309W was not kinetically characterized but aromaticity at this position was maintained with indole substitution for the phenol group. Maintenance of the junction between the small subsite and the leaving group subsite is apparently critical for hydrolysis of the thiophosphate targets (Figure 9). F132V/I106T and F132G/I106T hydrolyzed paraoxon more rapidly, FNT much more slowly and CPF at a similar rate compared to S308G/Y309W, with F132V/I106T the best among them for CPF hydrolysis (Table 4). Based on the kinetic profiles of these double mutants, the observed improvement in k_{cat} for paraoxon hydrolysis by I106T/F132V/S308A/Y309W is likely due to the F132V/I106T substitutions, while the rise in K_m appears to be caused by the S308A/Y309W mutations.

I106G and F132V point mutants were more reactive than any of the double mutants harboring these substitutions. I106T double mutants containing substitutions at position 132 were less reactive than the corresponding F132 point mutants with one exception: incorporation of I106T into an F132V variant improves paraoxon hydrolysis (Table 2). While none of the F132 point mutants had k_{cat}/K_m values in excess of the corresponding wild type values, glycine and valine substitution is well tolerated. S308G also hydrolyzed all of the targets more efficiently than S308G/Y309W. However, without kinetic characterization of the Y309W mutant the relative effect of each individual mutation is difficult to parse. Based on the profiles of the point mutants,

F132G, F132V, and S308G substitution appears to exhibit the smallest perturbation on active site chemistry.

Fenitrothion had a similar K_m value to paraoxon, but its k_{cat} value was ~50 fold lower. Passage through the active site after cleavage may be slowed by an additional amino acid contact. Slight enlargement of a binding pocket or at a corner between pockets could better accommodate the aromatic leaving group if the methyl group sterically hinders catalysis. Possible nitro group interactions with hydrogen bond donor R groups were probed via substitutions for S308 and Y309 to determine if transition state hydrogen bonding is rate limiting for product removal. While none of the active site mutants improved FNT hydrolysis, an unexpected result from the mutagenesis study could ultimately prove useful in determining binding. The S308T/F132V mutant undergoes substrate inhibition at concentrations above 100 μM (Table 5). Substrate soaking with this mutant may reveal alternate binding conformations in a crystal structure. While its leaving group is the most similar to p-nitrophenol, FNT was the only target for which substrate inhibition was observed. A dominant binding mode in a crystal structure could indicate an important interaction in the active site which is rate limiting for substrate hydrolysis.

Chlorpyrifos contains a trichloro-conjugated pyridine leaving group that has the lowest pKa of the three targets. Chlorpyrifos had the lowest K_m from the initial screen as well as the second lowest k_{cat} (Table 1). Hydrolysis of the phosphoryl ester bond generates an oxyanion that is delocalized into the pyridine ring. Given the largely hydrophobic nature of the active site, the electronegative chlorine atoms complicate

binding. I propose that a limited number of substrate orientations permit strong binding and the low k_{cat} and K_m are a reflection of this. The metal ions, which coordinate directly to the phosphoryl sulfur, are surrounded by the most polar binding pocket in the active site (Figure 7). The 3,4,6-chloro pyridine ring lacks a natural binding site and unfavorable release of this oxyanion product inhibits catalysis. F132 sits near the exit to the leaving group site and controls substrate stereoselectivity [30]. Replacement of this phenyl group with smaller R groups to permit a wider range of leaving group conformations was tested as a means of accelerating product release of the achiral substrates (Figure 8).

Valine substitution for F132 coupled with glycine substitution for S308 improved chlorpyrifos hydrolysis (Table 4). These two positions are on nearly opposite sides of the active site and do not interact. S308 is proposed to interact with the nascent leaving group. The hydroxyl group is one of the best hydrogen bond donors in the vicinity of the substrate binding site. Mutation to threonine, however, dramatically reduces reactivity with the targets. The additional methyl group likely restricts freedom of motion for the hydroxyl group. Conformational change following hydrolysis would reposition S308 to better accommodate transition state structures. Threonine's side group is likely locked into a position which is not amenable to conformational rearrangement.

The phenyl ring at position 132 is amenable to substitution with smaller alkyl side groups. Unlike Y309 and F306, aromaticity at this position is not essential for efficient catalysis. While F132G retains activity against all of the targets, S308G/F132G

was the least reactive double mutant purified. The additional conformational flexibility gained from glycine substitution at position 308 is believed to accelerate an early conformational change that may be rate limiting. However, glycine substitution at both positions removes substantial bulk from the active site and might allow unfavorable constriction of the leaving group site. The additional steric constraint from valine substitution at 132 compared to glycine substitution is expected to alter the conformational landscape. S308G mutation is predicted to accelerate a rate limiting conformational change by removing an interaction between the hydroxyl group and the pyridine leaving group. F132V mutation is predicted to affect transition state binding by increasing conformational flexibility. The polar leaving group for CPF may also interact with the pi system of the phenyl ring at position 132, slowing product removal. The alkyl side group of valine helps position transition state structures for product removal in the absence of the potential electrostatic interaction with the benzene ring.

Coumaphos had by far the highest k_{cat} and the second lowest K_m of the substrates tested in the initial screen. The low K_m relative to paraoxon is particularly interesting given the difference in size between the coumarin ring and p-nitrophenol. A computationally redesigned enzyme which readily hydrolyzes organophosphates with coumarinyl leaving groups but not paraoxon was recently characterized [39]. The active site architecture in the redesigned zinc adenosine deaminase apparently accommodates this non-cognate reaction via leaving group activation. The authors postulate that nonproductive binding of smaller substrates could account for the loss of enzymatic reactivity. Proper alignment for catalysis upon initial binding is a possible explanation

for the low Michaelis constant for coumaphos hydrolysis. Each of the targets contains achiral thiophosphate heads. Steric constraint from the coumarin ring may restrict spatial arrangement of the phosphate R groups at the phosphate-binding moiety and reduce unproductive binding in the wild type enzyme. Enlargement of the leaving group site via substitution of F132 was unsuccessfully tested as a means of aiding removal of the bulky coumarin ring.

CHAPTER V

SUMMARY AND CONCLUSIONS

Substitutions within the active site were introduced at suspected conformational "hotspots" to aid product removal. Identification of suitable positions for mutagenesis was deduced largely from directed evolution studies with paraoxon, chlorpyrifos or coumarinyl analogue selection. Point mutants at 3 positions of interest, I106, S308 and F132, were initially characterized to determine the importance of amino acid side group identity at these positions. Seven active site double mutants: F132G/S308G, F132G/S308T, F132V/S308G, F132V/S308T, F132G/I106T, F132V/I106T and G308/W309 were purified to homogeneity for kinetic characterization, with one of these mutants, F132V/S308G, exhibiting improved reactivity compared to the wild type enzyme against chlorpyrifos. Acceleration of two potential rate limiting steps, early conformational change following hydrolysis and product removal, was tested as a means of increasing reactivity.

Substitution at position 308 should be restricted to alanine and glycine in order to retain activity. Threonine substitution abolishes activity, which indicates that R group identity at this position may not be as important as flexibility. All of the targets contained aromatic alcohol leaving groups. Y309 and F306 are important for leaving group positioning. The finding that T308 substitution reduces reactivity by over an order of magnitude with some targets and in fact introduces substrate inhibition in

another (FNT) was an unexpected result. Reactivity after mutation at this position appears to depend more on size than hydrogen bonding capability.

Future work may make use of substitution for the phenyl ring at position 132 as a means of testing product removal as a rate limiting step. Of the 4 leaving group residues identified in PTE, position 132 is the most amenable to substitution. Glycine and valine point mutants at this position retained activity with all targets. Previous mutagenic study identified F132 as the residue which controls stereoselectivity. This control could be exhibited via conformational change or simply through sterics. Position 132 is predicted to exert influence over transition state binding and orientation within the active site. Aromaticity was removed from this position to facilitate rapid removal of the aromatic alcohol leaving groups by eliminating a potential electrostatic interaction. Elimination of the bulky phenyl ring opens the active site and is predicted to increase conformational freedom. Restricting conformational closing of the leaving group site as was postulated for the F132G/S308G double mutant is critical for catalysis.

Combining mutations on opposite sides of the active site in PTE does not abolish activity, while substitution of neighboring residues distorts the active site architecture in a detrimental fashion. At the pH used for all kinetic reactions, conformational change and/or product removal is rate limiting. The dominant conformations during catalysis remain to be elucidated, but this study provides evidence that F132 and S308 may control conformational change. Additional points of control for conformational change have been identified in distal residues, but within the active site these residues appear to be unique due to their importance for structural rearrangement.

REFERENCES

1. Lopez-Munoz, F., P. Garcia-Garcia, and C. Alamo, *The pharmaceutical industry and the German National Socialist Regime: I.G. Farben and pharmacological research.* Journal of clinical pharmacy and therapeutics, 2009. **34**(1): p. 67-77.

2. Freeman, S.E., *Present state of control of chemical and biological weapons.* Medicine and war, 1991. **7**(1): p. 16-20.

3. Gorka, S., *Biological weapons and the pharmaceutical industry.* International journal of pharmaceutical medicine, 2000. **14**(4): p. 213-218.

4. Munnecke, D.M., *Enzymatic hydrolysis of organophosphate insecticides, a possible pesticide disposal method.* Applied and environmental microbiology, 1976. **32**(1): p. 7-13.

5. Benning, M.M., et al., *Three-dimensional structure of phosphotriesterase: an enzyme capable of detoxifying organophosphate nerve agents.* Biochemistry, 1994. **33**(50): p. 15001-7.

6. Raushel, F.M., *Chemical biology: Catalytic detoxification.* Nature, 2011. **469**(7330): p. 310-1.

7. Bondarenko, S., et al., *Persistence of selected organophosphate and carbamate insecticides in waters from a coastal watershed.* Environmental toxicology and chemistry / SETAC, 2004. **23**(11): p. 2649-54.

8. James, R.R. and J. Xu, *Mechanisms by which pesticides affect insect immunity.* Journal of invertebrate pathology, 2012. **109**(2): p. 175-82.

9. Michal Alon a, F.A.a., Ralf Nauen b, Shai Morin a,*, *Organophosphates' resistance in the B-biotype of Bemisia tabaci (Hemiptera: Aleyrodidae) is associated with a point mutation in an ace1-type acetylcholinesterase and overexpression of carboxylesterase.* 2008.

10. Gao, J.R. and K.Y. Zhu, *Comparative toxicity of selected organophosphate insecticides against resistant and susceptible clones of the greenbug, Schizaphis graminum (Homoptera: aphididae).* Journal of agricultural and food chemistry, 2000. **48**(10): p. 4717-22.

11. Hong, S.B. and F.M. Raushel, *Metal-substrate interactions facilitate the catalytic activity of the bacterial phosphotriesterase.* Biochemistry, 1996. **35**(33): p. 10904-12.

12. Tsai, P.C., et al., *Stereoselective hydrolysis of organophosphate nerve agents by the bacterial phosphotriesterase.* Biochemistry, 2010. **49**(37): p. 7978-87.

13. Lai, K., N.J. Stolowich, and J.R. Wild, *Characterization of P-S bond hydrolysis in organophosphorothioate pesticides by organophosphorus hydrolase.* Archives of biochemistry and biophysics, 1995. **318**(1): p. 59-64.

14. *Prevention, Pesticides And Toxic Substances*, U.E.P. Agency, Editor 1996.

15. Yan, C., et al., *Repeated exposures to chlorpyrifos lead to spatial memory retrieval impairment and motor activity alteration.* Neurotoxicology and teratology, 2012. **34**(4): p. 442-449.

16. *Prevention, Pesticides And Toxic Substances*, U.E.P. Agency, Editor 2002.

17. Mugni, H., et al., *Toxicity persistence in runoff water and soil in experimental soybean plots following chlorpyrifos application.* Bulletin of environmental contamination and toxicology, 2012. **89**(1): p. 208-12.

18. Sarikaya, R., et al., *The acute toxicity of fenitrothion on narrow-clawed crayfish (Astacus leptodactylus Eschscholtz, 1823) in association with biomarkers of lipid peroxidation.* Journal of biochemical and molecular toxicology, 2011. **25**(3): p. 169-74.

19. *Prevention, Pesticides And Toxic Substances*, U.E.P. Agency, Editor 2000.

20. Livingstone, D.R., *Contaminant-stimulated reactive oxygen species production and oxidative damage in aquatic organisms.* Marine pollution bulletin, 2001. **42**(8): p. 656-66.

21. Lewis, V.E., et al., *Mechanism and stereochemical course at phosphorus of the reaction catalyzed by a bacterial phosphotriesterase.* Biochemistry, 1988. **27**(5): p. 1591-7.

22. Jackson, C., et al., *The structure of an enzyme-product complex reveals the critical role of a terminal hydroxide nucleophile in the bacterial phosphotriesterase mechanism.* Biochimica et biophysica acta, 2005. **1752**(1): p. 56-64.

23. Aubert, S.D., Y. Li, and F.M. Raushel, *Mechanism for the hydrolysis of organophosphates by the bacterial phosphotriesterase.* Biochemistry, 2004. **43**(19): p. 5707-15.

24. Chen, S.L., W.H. Fang, and F. Himo, *Theoretical study of the phosphotriesterase reaction mechanism.* The journal of physical chemistry. B, 2007. **111**(6): p. 1253-5.

25. Vanhooke, J.L., et al., *Three-dimensional structure of the zinc-containing phosphotriesterase with the bound substrate analog diethyl 4-methylbenzylphosphonate.* Biochemistry, 1996. **35**(19): p. 6020-5.

26. Hong, S.B. and F.M. Raushel, *Stereochemical constraints on the substrate specificity of phosphotriesterase.* Biochemistry, 1999. **38**(4): p. 1159-65.

27. Jackson, C.J., et al., *Conformational sampling, catalysis, and evolution of the bacterial phosphotriesterase.* Proceedings of the National Academy of Sciences of the United States of America, 2009. **106**(51): p. 21631-6.

28. Musilek, K., et al., *Design, evaluation and structure-activity relationship studies of the AChE reactivators against organophosphorus pesticides.* Medicinal research reviews, 2011. **31**(4): p. 548-75.

29. Griffiths, A.D. and D.S. Tawfik, *Directed evolution of an extremely fast phosphotriesterase by in vitro compartmentalization.* The EMBO journal, 2003. **22**(1): p. 24-35.

30. Chen-Goodspeed, M., et al., *Structural determinants of the substrate and stereochemical specificity of phosphotriesterase.* Biochemistry, 2001. **40**(5): p. 1325-31.

31. Briseno-Roa, L., et al., *Highest paraoxonase turnover rate found in a bacterial phosphotriesterase variant.* Protein engineering, design & selection : PEDS, 2011. **24**(1-2): p. 209-11.

32. Nagano, N., C.A. Orengo, and J.M. Thornton, *One fold with many functions: the evolutionary relationships between TIM barrel families based on their sequences, structures and functions.* Journal of molecular biology, 2002. **321**(5): p. 741-65.

33. Harper, L.L., et al., *Dissimilar plasmids isolated from Pseudomonas diminuta MG and a Flavobacterium sp. (ATCC 27551) contain identical opd genes.* Applied and environmental microbiology, 1988. **54**(10): p. 2586-9.

34. Liang, B., et al., *Facilitation of bacterial adaptation to chlorothalonil-contaminated sites by horizontal transfer of the chlorothalonil hydrolytic dehalogenase gene.* Applied and environmental microbiology, 2011. **77**(12): p. 4268-72.

35. Mee-Hie Cho, C., A. Mulchandani, and W. Chen, *Functional analysis of organophosphorus hydrolase variants with high degradation activity towards organophosphate pesticides.* Protein engineering, design & selection : PEDS, 2006. **19**(3): p. 99-105.

36. Cho, C.M., A. Mulchandani, and W. Chen, *Altering the substrate specificity of organophosphorus hydrolase for enhanced hydrolysis of chlorpyrifos.* Applied and environmental microbiology, 2004. **70**(8): p. 4681-5.

37. Benning, M.M., et al., *High resolution X-ray structures of different metal-substituted forms of phosphotriesterase from Pseudomonas diminuta.* Biochemistry, 2001. **40**(9): p. 2712-22.

38. Kuo, J.M., M.Y. Chae, and F.M. Raushel, *Perturbations to the active site of phosphotriesterase.* Biochemistry, 1997. **36**(8): p. 1982-8.

39. Khare, S.D., et al., *Computational redesign of a mononuclear zinc metalloenzyme for organophosphate hydrolysis.* Nature chemical biology, 2012. **8**(3): p. 294-300.